Seasonal dynamics of zooplankton nutrient recycling in a hypereutrophic reservoir

Tyler J. Butts[1,3*], Eric K. Moody[2], Grace M. Wilkinson[1,3]
[1]Ecology, Evolution and Organismal Biology Department, Iowa State University, Ames, IA
[2]Department of Biology, Middlebury College, Middlebury, VT
[3]Current Address: Center for Limnology, University of Wisconsin – Madison, Madison, WI

***Corresponding Author:**
Tyler Butts
tjbutts@wisc.edu

Key Words: nutrient cycling, stoichiometry, hypereutrophic, body size, excretion

ABSTRACT

Consumer-driven nutrient cycling influences aquatic ecosystem functioning by altering energy flow as well as the movement and transformation of nutrients. In hypereutrophic lakes, zooplankton nutrient recycling has largely been considered negligible due to the high concentrations of available nutrients. A recent comparative analysis found that zooplankton community composition may influence nutrient availability, particularly phosphorus availability, in hypereutrophic lakes. However, the magnitude and timing of the effect of zooplankton nutrient recycling and grazing on phytoplankton in hypereutrophic lakes remains unclear. We quantified zooplankton, phytoplankton, and nutrient concentration dynamics during the summer of 2019 in a temperate, hypereutrophic reservoir. We found that zooplankton excretion contributed a substantial proportion (23-46%) to the inorganic phosphorus (P) pool in early summer when P concentrations were low and limiting phytoplankton growth. Zooplankton excretion of P also significantly (p=0.003) contributed to variation in phytoplankton community composition in early summer. Further, we found evidence that zooplankton affected phytoplankton size distributions through selective grazing of smaller phytoplankton cells. Overall, our results demonstrate the important role of zooplankton in hypereutrophic lakes as excretion helped drive springtime phytoplankton dynamics through nutrient recycling while grazing influenced phytoplankton size distributions later in the summer.

INTRODUCTION

Animal consumers drive nutrient cycling in aquatic ecosystems by controlling the movement and transformation of nutrients over time and across space (Atkinson *et al.*, 2017). Aquatic consumers such as zooplankton ingest primary producers then excrete and egest metabolized and unassimilated materials as waste, recycling nutrients back into the ecosystem (Vanni, 2002). In turn, these excreted, recycled nutrients can be taken up by phytoplankton to produce new biomass (Sarnelle and Knapp, 2005). Mismatches between consumer demand for and assimilation efficiency of elements and the elemental composition of primary producers drives the stoichiometry of nutrients recycled back into the ecosystem (Elser and Hassett, 1994; Sterner, 1990). Elemental mismatches can then lead to greater nutrient recycling of a particular element that may result in changes to ecosystem nutrient limitation and alter trophic interactions between consumers and their resource (Elser *et al.*, 2000; Dobberfuhl and Elser, 2000).

The community composition of both phytoplankton and zooplankton can influence the stoichiometry of recycled nutrients and generate strong differences in nitrogen (N) and phosphorus (P) recycling (Balseiro *et al.*, 1997). For example, copepods and small cladocerans generally retain more N whereas *Daphnia* generally retain more P (Elser and Urabe, 1999). Differences in N and P retention between zooplankton taxa can result in copepod and small cladoceran dominated communities retaining more N and recycling more P into the water column, thereby driving phytoplankton to N-limitation (Elser *et al.*, 2000, 1988). Phytoplankton community composition varies with lake trophic state and nutrient limitation as different phytoplankton genera prefer different nutrient forms (Andersen *et al.*, 2020). Cyanobacteria-dominated phytoplankton communities, which often arise in nutrient enriched ecosystems, are uniquely resistant to zooplankton grazing due to the ability of many genera to form colonies or filaments, as well as their poor nutritional quality, toxin production and rapid growth rates (Moustaka-gouni and Sommer, 2020). This results in a loss of nutrient and energy transfer to higher trophic levels due to poor assimilation efficiency (Karpowicz *et al.*, 2021, 2020). In combination, zooplankton-phytoplankton interactions affect nutrient recycling in aquatic ecosystems; however, the effects may vary depending on the severity of nutrient enrichment.

Much of our understanding regarding zooplankton nutrient recycling comes from oligotrophic and eutrophic ecosystems (Elser *et al.*, 2000; Moegenburg and Vanni, 1991), though many temperate lakes are increasingly becoming hypereutrophic due to continued land use conversion and climate change (Stoddard *et al.*, 2016). The extremely high nutrient concentrations in hypereutrophic lakes can produce unique conditions compared to less enriched waterbodies such as large seasonal variability in nutrient limitation of phytoplankton growth (Andersen *et al.*, 2020), substantial internal phosphorus loading under oxic conditions (Song and Burgin, 2017), and a more complex mix of top-down and bottom-up forces affecting phytoplankton communities (Matsuzaki *et al.*, 2018). However, the contribution of zooplankton nutrient recycling in hypereutrophic ecosystems is often considered negligible as high concentrations of inorganic nutrients within the water column can dampen the influence of nutrient inputs from consumer excretion (Spooner *et al.*, 2013). Despite this, zooplankton may still influence nutrient availability in hypereutrophic lakes as nutrient limitation and zooplankton biomass shift throughout the growing season. Additionally, selective feeding on small phytoplankton by small-bodied zooplankton increases the dominance of large phytoplankton species, including filamentous and colonial cyanobacteria (Erdoğan *et al.*, 2021). This may influence nutrient availability as cyanobacteria have the capacity for luxury nutrient uptake, subsequent storage of excess nutrients, and the ability to use N forms inaccessible to other phytoplankton species, such as diazotrophs that can fix atmospheric nitrogen (Cottingham *et al.*, 2015). As hypereutrophic lakes are dominated by smaller-bodied zooplankton including microzooplankton and ciliates, selective grazing pressure on the phytoplankton community may indirectly influence nutrient availability.

A recent analysis of mesozooplankton (i.e., copepods, cladocerans, and rotifers; hereafter zooplankton) stoichiometric traits found that the community N:P ratio shifted towards N-rich species with increasing eutrophication (Moody and Wilkinson, 2019). As such, in hypereutrophic lakes, zooplankton may be increasing P recycling. This hypothesis was supported by the fact that the seston N:P in hypereutrophic lakes was lower compared to less enriched lakes concurrent with more N-rich zooplankton communities that exhibit greater P recycling. This analysis suggests that the unique functioning of hypereutrophic lakes, even compared to eutrophic lakes, was due in part to the consumers inhabiting them. However, this was a comparative study among lakes based on a single sampling point in summer. It is well established that zooplankton and phytoplankton communities are dynamic and undergo an annual succession over the course of a summer growing season, which can vary depending on lake trophic state and other variables (Sommer *et al.*, 2012). Furthermore, the balance of top-down and bottom-up forces in lakes varies with nutrient ratios and concentrations across a season (Rogers *et al.*, 2020). In the scope of this comparative study (Moody and Wilkinson, 2019), the seasonal variability within zooplankton, phytoplankton, and nutrient dynamics was not captured. As such, it remains unclear how hypereutrophic lakes are influenced by zooplankton nutrient recycling throughout the summer growing season.

We investigated the role of zooplankton nutrient recycling in a hypereutrophic waterbody by quantifying zooplankton, phytoplankton, and water column nutrient dynamics across the summer growing season. We used effect traits, which directly link individual activity to ecosystem processes (Hébert *et al.*, 2017, 2016b), to estimate storage and flux of nutrients driven by zooplankton consumers. Effect traits like size (Litchman *et al.*, 2013) or elemental composition (Sterner and Elser, 2002) can be used to assess nutrient cycling by quantifying zooplankton body stoichiometry and excretion rate, as well as to infer growth and predation based on community body size structure. With this approach we asked: (1) do zooplankton in hypereutrophic lakes alter P availability, and how does that vary over the course of a summer growing season? And (2) do zooplankton contribute to variation in phytoplankton community composition amidst other environmental variables? We hypothesized that zooplankton nutrient recycling would contribute to P availability before the onset of high internal P loading in midsummer. Furthermore, we expected zooplankton excretion would contribute to variation in phytoplankton community composition due to body stoichiometry shifting nutrient availability. Finally, we hypothesized that zooplankton grazing would affect phytoplankton size structure throughout the summer due to selective grazing on smaller phytoplankton.

METHODS

Study Lake

Green Valley Lake (46°06’02” N, 94°23’05” W) is a hypereutrophic reservoir built in 1952 as an impoundment of the Platte River in southwestern Iowa (USA). The maximum depth is 7.3 m, with an average depth of 3.2 m and a surface area of 156 ha. The fish community is dominated by crappie (*Pomoxis spp.)*, bluegill (*Lepomis macrochirus*), and largemouth bass (*Micropterus salmoides*). Additionally, there is a small population of common carp (*Cyprinus carpio*) and channel catfish (*Ictalurus punctatus*). The watershed is dominated by row crop agriculture (68.4% corn/soybean rotation). Consequently, Green Valley Lake is enriched with nutrients and beset by annual phytoplankton blooms dominated by cyanobacteria (Supplementary Figure S1). To characterize zooplankton nutrient recycling in Green Valley Lake, zooplankton, phytoplankton, and water samples for nutrient analysis were taken weekly at the deepest point in the reservoir during the summer of 2019. Samples were taken from early May (day of year; DOY 143) to early September (DOY 251). An additional sampling event occurred on DOY 273, but only zooplankton and nutrient samples were collected at that time. Additionally, a YSI EXO3 sonde (Yellow Springs Instruments, Yellow Springs, Ohio, USA) was deployed at 0.5 m at the deepest point in the reservoir and collected temperature, total dissolved solids, and pH measurements every 15 minutes. Daily averages of each variable were used in our analyses.

Plankton Analysis

Zooplankton and phytoplankton biomass and community composition were quantified for each sampling event during the summer growing season. Zooplankton were sampled via a vertical tow of a Wisconsin net (63 µm mesh) from 6 m depth. Samples were preserved with a formaldehyde solution (5% concentration after sample addition) in the field and later transferred to 70% ethanol. Phytoplankton samples were a composite sample over depth. Water was collected in a 4 L Van Dorn sampler from 0.25, 1, 2, 3, and 4 m depths, then mixed in a 20 L carboy in the field. Samples were taken to 4 m depth which was the average thermocline depth at the sampling point (4.0 ± 1.23 m; s.d.). A 1 L sample was then taken from the carboy following thorough mixing and preserved with Lugol's solution in the field.

Zooplankton samples were identified and enumerated with a Leica MZ8 stereomicroscope connected to Motic Images software. For each sample a 1 mL subsample was taken where a minimum of 60 individual zooplankton were identified and enumerated. If less than 60 organisms were in the subsample a second 1 mL subsample was counted. Individuals were identified to genus for cladocerans and rotifers, order for copepods, and class for ostracods. Copepod nauplii could not be identified to order and were simply identified as nauplii. We measured zooplankton lengths to calculate dry mass per liter using length-weight regressions (Dumont *et al.*, 1975; McCauley, 1984). For visual display of the zooplankton data, they were separated into nine taxonomic groups: *Daphnia, Simocephalus, Ceriodaphnia*, *Bosmina, Chydorus*, rotifers, calanoids, cyclopoids, nauplii, and ostracods (Supplementary Table S1).

Simocephalus contributed only 7% of total community biomass at its peak biomass and so were grouped with *Daphnia* for later analyses.

The 1 L phytoplankton samples were transferred to a graduated cylinder and allowed to settle in a dark environment for 8 days before the supernatant was removed with a vacuum pump, leaving 50 mL of concentrated sample. A subsample was then removed from the concentrated sample and identified and enumerated using a modified Palmer-Maloney chamber. Phytoplankton were identified to genus and measured using a calibrated ocular reticle on a Leitz DM IL inverted microscope at 400x magnification. A minimum of 300 natural units across 8 fields were measured for each sample. Biovolume per liter was calculated based on phytoplankton shape and then converted to wet biomass per liter assuming a 1:1 ratio between wet mass and biovolume (Hillebrand *et al.*, 1999; Sournia, 1978). Like zooplankton, phytoplankton genera were separated into six groups for visual display: bacillariophytes, chlorophytes, chryso- and cryptophytes, *Aphanothece*, *Microcystis,* and other cyanophytes (Supplementary Table S2). Both *Aphanothece* and *Microcystis* were the dominant genera of cyanobacteria, contributing the majority of phytoplankton biomass (88 ± 18%; s.d.) and therefore were visualized separately.

Nutrient Analysis

To quantify the concentration and forms of nutrients in Green Valley Lake, surface water samples were collected at a depth of 0.25 m at the deep point. A subset of the water was first filtered through Whatman glass fiber filters (pore size = 0.45 µm) in the field, preserved with concentrated sulfuric acid to a pH of 2, and stored at 4 ºC until analysis for soluble reactive phosphorus (SRP) and nitrate + nitrite (NOx). Unfiltered sample water was preserved with concentrated sulfuric acid to a pH of 2 and stored at 4 ºC until analysis for total phosphorus (TP) and total nitrogen (TN). The ascorbic acid method was used to quantify P concentrations with filtered water for SRP and unfiltered water that had undergone persulfate digestion for TP. Second-derivative ultraviolet spectroscopy was used to quantify NOx concentrations in filtered samples and TN concentrations following persulfate digestion. N species were analyzed using an Agilent Cary 8454 UV-VIS spectrophotometer (Agilent Technologies Inc, Santa Clara, CA, USA) and P species were analyzed using a Seal Analytical AQ2 Discrete Analyzer (Seal

Analytical Inc. Mequon, WI, USA). For data analysis, nutrient concentrations below detection were replaced with the instrument long-term method detection limit.

To investigate zooplankton nutrient recycling between different nutrient pools we quantified the available concentrations of nitrogen (N) and phosphorus (P) as well as calculated total and inorganic N and P. Nutrient limitation of phytoplankton was determined by the N:P ratio of total N and P with N:P > 20 indicating P limitation (Guildford and Hecky, 2000). A decade of summertime measurements of NHx in Green Valley Lakes indicates that it is rarely detectable (Supplementary Material).

Zooplankton Stoichiometry and Excretion

To assess the contribution of zooplankton to nutrient availability we determined zooplankton elemental composition, nutrient storage, and excretion rate. We estimated elemental composition and total nutrient storage by zooplankton (L^{-1} d-^{1}) following methods described previously (Moody and Wilkinson, 2019). Briefly, taxa-specific %N and %P collected from the literature (Hamre, 2016; Hébert *et al.*, 2016a; Hessen *et al.*, 2007) were used to estimate total nutrient storage by multiplying %N and %P by the biomass of each taxa and summing across the community on each sampling date. Although we are using trait data from largely oligotrophic lakes, zooplankton express fairly strong stoichiometric homeostasis (Persson *et al.*, 2010) as well as low intraspecific stoichiometric variation between lakes (Prater *et al.*, 2017) and variable food quality (Teurlincx *et al.*, 2017). Thus, it is unlikely that intraspecific variation in %N and %P values in our study lake will have a large influence.

Excretion rates of N and P by zooplankton were estimated using published allometric equations (Supplementary Material). The equations relate zooplankton body size to N and P excretion rates derived from a compiled dataset of marine and freshwater zooplankton species (Hébert *et al.*, 2016b, 2016a). Briefly, for each sampling event we input the average dry mass per zooplankton taxon into the allometric equations to determine individual N and P excretion rates (μM N or P individual^{-1} hour^{-1}) then converted the hourly excretion rate to a daily rate (day^{-1}). Next, we multiplied the daily excretion rates by the density of each taxon (individuals L^{-1}), then summed the excretion rates across taxa to calculate a zooplankton community excretion on that sampling date (μM N or P day^{-1}). We calculated uncertainty in the excretion estimates by propagating the variation in the slope and intercept from the allometric equations presented in

Hébert *et al.*, (2016b). We also calculated zooplankton excretion using other published allometric equations from Wen and Peters (1994) that were derived from different underlying datasets. The overall pattern of zooplankton excretion did not differ between the two methods; however, the Wen and Peters (1994) based estimates of excretion were slightly higher (Supplementary Table S3). We chose to use the more conservative estimate of zooplankton excretion rates based on Herbert et al. (2016) in our analysis as the method also allowed us to estimate uncertainty.

Data Analysis

To assess the magnitude of zooplankton N and P excretion in Green Valley Lake we compared the estimated concentration of excreted N and P over the course of a day to the measured surface water concentrations of inorganic N and P for each sampling event. This was expressed as a percent of the inorganic nutrient pool:

$$\left(\frac{\mu M\ N\ or\ P\ excreted\ by\ zooplankton\ community\ in\ a\ day}{\mu M\ of\ inorganic\ N\ or\ P\ present\ in\ the\ surface\ waters}\right) * 100 \qquad (1)$$

To assess how zooplankton affected the rate of nutrient cycling over the course of the growing season we calculated the zooplankton nutrient turnover time of the inorganic P pool. Turnover, in this case, is the number of days it would take for zooplankton excretion of P, estimated for a specific sampling date to reach the concentration SRP measured on the same sampling date, assuming no uptake from phytoplankton (SRP/excretion rate). The turnover time varies depending on the rate of zooplankton excretion and concentration of SRP in the surface waters. We did not have a weekly measurement of ammonium as it was likely undetectable based on previous monitoring, so we could not calculate turnover of the soluble N pool. Short turnover times of inorganic P indicate zooplankton are significantly contributing to the inorganic P pool in Green Valley Lake. Long nutrient turnover times indicate factors other than zooplankton excretion are driving nutrient availability.

To assess the drivers of phytoplankton community composition across the growing season we performed a distance based-redundancy analysis (db-RDA). In order to ascertain whether zooplankton nutrient recycling partially explained phytoplankton community composition we included zooplankton excretion and body stoichiometry with other potentially important environmental variables including inorganic nutrient concentration (Filstrup and Downing, 2017), temperature (Striebel *et al.*, 2016)**,** pH (Rönicke *et al.*, 2010), and total dissolved solids (Ahmed and Wanganeo, 2015). Phytoplankton species biomass data were Hellinger transformed and species that only occurred once in the full summer dataset and contributed <1% of total biomass were removed to decrease the weight of rare species. Environmental variables were z-scored in order to correct for differences in scale and magnitude (Legendre and Legendre, 1998). The db-RDA was performed using a Bray-Curtis distance matrix using the square roots of dissimilarities to avoid negative eigenvalues (Legendre and Anderson, 1999). Missing or lost samples were removed from the final analysis. The best model was determined using forward and backward stepwise regression with model significance determined using a Monte Carlo permutation test (999 permutations, p-value < 0.05).

To investigate the importance of zooplankton top-down control we calculated the percentage of zooplankton biomass to phytoplankton biomass. The percentage of zooplankton biomass in comparison to phytoplankton biomass has been used as a proxy for describing the importance of top-down v. bottom-up control in lakes, with a high percentage (~40-50%) indicating strong top-down control and a low percentage (~10%) indicating weak top-down control (Leroux and Loreau, 2015; Havens and Beaver, 2013). Additionally, we compared the size distributions of zooplankton and phytoplankton communities and individual zooplankton mass, as well as their changes over time. Zooplankton length data were compiled for up to 25 individuals per taxa per sampling date then used to estimate body mass with taxa-specific length-weight regressions (Dumont *et al.*, 1975; McCauley, 1984). When more than 25 individuals of a species were present in a sample, the total number was counted, but length was only measured for the first 25 individuals. The greatest axial linear dimension (GALD) of phytoplankton was measured as the greatest distance across an individual cell, colony, or filament (i.e., natural unit), such as would be encountered by a zooplankton grazer. Distributions of zooplankton length and body mass were compared to the distribution of phytoplankton GALD for each sampling date to investigate the size distribution dynamics over time in the two trophic levels. Additionally, we performed a linear regression of mean phytoplankton GALD versus mean zooplankton size. All analyses were performed using the statistical software R version 4.0.4 (R Core Team, 2021) with the, *magrittr*, and *vegan* packages (Bach and Wickham, 2020; Oksanen *et al.*, 2020).

RESULTS

First, we assessed zooplankton and phytoplankton community composition and biomass during the summer growing season. Zooplankton biomass peaked (249 µg L^{-1}) in late May and early June (DOY 150-164), rapidly decreased to its minimum (~2 µg L^{-1}) in mid-July to late August (DOY 192 – DOY 234), then returned to early summer concentrations through September (Figure 1A). The early summer zooplankton community was dominated by *Daphnia* and calanoid copepods which transitioned in early July (DOY 199) to a community dominated by *Chydorus* and cyclopoid copepods, then transitioning back to *Daphnia* in late August (Figure 1A). Zooplankton top-down control was very low (<10%) over the course of the growing season with the percentage of zooplankton biomass to phytoplankton biomass peaking on DOY 164 at 6.9%. Similar to zooplankton biomass, phytoplankton biomass was initially high in the spring, mainly composed of bacillariophytes, before rapidly decreasing during the clear-water period between DOY 150 – 164 when zooplankton biomass was at its highest (Figure 1B). Following DOY 172, the phytoplankton community was overwhelmingly composed of cyanophytes, mainly *Microcystis*, with phytoplankton reaching peak biomass on DOY 213 (~329 mg L^{-1}). The other dominant cyanophyte was the diazotroph *Aphanothece*, which was present from DOY 192 – 228.

Nutrient concentrations and limitation were dynamic throughout the summer (Figure 2). Inorganic N concentrations were highest in the spring and decreased by 80% to low or undetectable concentrations after DOY 178 (Figure 2A). At the same time, there was a rapid increase in inorganic P of 394% from DOY 172 to 178 and a 937% increase from DOY 178 to DOY 206 (Figure 2B). The storage of N in zooplankton biomass was negligible over the course of the growing season (Figure 2A), however P storage nearly equaled inorganic P concentrations in the water column early in the summer when zooplankton biomass peaked (Figure 2B). Total N:P declined rapidly in mid-July (DOY 192), transitioning the ecosystem from P- to intermittent N-limitation. There was also a shift in inorganic N:P to N-limitation in mid-July that was persistent for the remainder of the summer (Figure 2C). Zooplankton community body N:P was the highest in mid-summer, coincident with the rapid transition between P- and N-limitation, then steadily declined throughout the rest of the sampling period (Figure 2D).

Supporting our hypothesis, zooplankton excretion contributed substantially to the inorganic P pool from late May to late June (DOY 143-172), with daily excretion ranging between 23-46% of the inorganic P standing stock (Figure 3). Following DOY 172, the contribution of zooplankton excretion to the inorganic P pool dropped below 1% for the remainder of the sampling period. Furthermore, zooplankton excretion was contributing to a rapid turnover of the inorganic P pool in early summer with turnover times ranging between 3 – 4 days but increased well beyond 365 days as inorganic P concentrations increased in late June (Supplementary Table S4). Estimated zooplankton N excretion was never more than 3.3% of the inorganic N pool over the course of the growing season (Figure 3).

In support of our second hypothesis, the daily mass of zooplankton excretion significantly explained variance in phytoplankton community composition during early summer (DOY 143 – 164, Figure 4, Table 1). We found that the db-RDA discriminated the phytoplankton community into distinct communities defined by pre- and post-cyanobacterial dominance (F=2.44, p=0.003). A suite of environmental variables explained 41.9% of the variation in phytoplankton community composition including inorganic P (p=0.003) and N (p=0.020) concentrations, zooplankton P excretion (p=0.004), temperature (p=0.032), and total dissolved solids (p=0.046). Phytoplankton community composition was correlated with total dissolved solids, zooplankton N and P excretion, and inorganic N concentrations in early summer prior to the cyanobacteria bloom beginning on DOY 172 where phytoplankton community composition became more correlated with inorganic P concentrations and temperature. However, the significant axes did not explain a large proportion of the variation with the first axis explaining 28.4% and the second axis explaining only 13.4% of variation.

Furthermore, there was evidence that zooplankton were influencing the size distribution of phytoplankton GALD in mid- to late summer. There was a higher average GALD when mean zooplankton length was at its lowest (Figure 5A), and the density of smaller zooplankton individuals began increasing relative to the total size distribution in early June (DOY 164). Small individual zooplankton dominated the zooplankton size distribution from late June to early August (DOY 178 – 213). This was concurrent with a period in which larger phytoplankton dominated the GALD distribution (Figure 5A). Phytoplankton average GALD was greatest in July (mean = 32.5 ± 19.6 µm; s.d.) concurrent with the period of the summer where zooplankton average length was at its lowest (mean = 171 ± 102 µm; s.d.). In late July through August the difference in zooplankton length and phytoplankton GALD steadily increased, surpassing the mean differences observed in early summer (Figure 5B). A similar pattern was observed between phytoplankton GALD and zooplankton dry mass (Supplementary Figure S2). There was a weak negative relationship between GALD and zooplankton length (*p*=0.0119, R^2=0.42; Supplementary Figure S3A), and zooplankton body mass (*p*=0.0306, R^2=0.33; Supplementary Figure S3B).

DISCUSSION

Effect of zooplankton excretion on nutrient availability

We found that zooplankton excretion contributed substantially to the inorganic P pool in Green Valley Lake, but only during the early summer (DOY 143 – 178). It was during this period that inorganic P was at low concentrations in the water column and phytoplankton growth was likely P-limited, indicating that zooplankton-mediated recycling contributed to meeting nutrient demand by phytoplankton during this time. This early-season P availability, facilitated by zooplankton recycling, may have helped initialize the cyanotoxin-producing cyanobacteria bloom that flourished later in the season and persisted until late summer (Isles and Pomati, 2021). The large contribution of zooplankton to inorganic P availability is consistent with the hypothesis from Moody and Wilkinson (2019) that N-rich zooplankton communities, characteristic of hypereutrophic lakes, contribute to increased P availability within nutrient-rich ecosystems. Our study in Green Valley Lake, however, revealed that this zooplankton-mediated flux of P is mainly confined to the early part of the growing season.

Beginning on DOY 178, the concentration of inorganic P in Green Valley Lake increased substantially, diminishing the importance of zooplankton-recycled P, and driving the ecosystem to co-limitation or N-limitation for the rest of the season. The transition between P and N-limitation or co-limitation is a dynamic that has been reported in other eutrophic and hypereutrophic ecosystems (Andersen *et al.*, 2020; Wang *et al.*, 2019). The transition is likely a result of increased internal P loading (Albright and Wilkinson, 2022) and differences in N uptake strategies and preferences in the phytoplankton community, particularly when cyanobacteria begin to dominate (Li *et al.*, 2020; Glibert *et al.*, 2016). Furthermore, our estimates of P turnover by zooplankton indicated rapid turnover of inorganic pools during early summer, but drastically slowed once inorganic P concentrations rose. These results support our conclusions that zooplankton nutrient recycling was an important P flux during the early summer growing season, but not an important flux once internal loading increased P availability. Additionally, it is unlikely zooplankton had much influence over the turnover of total P and N across the entire summer, likely due to the lack of top-down control by the zooplankton community on phytoplankton throughout the summer growing season.

Overall, the contribution of zooplankton-recycling to the inorganic N pool in Green Valley Lake was never greater than 5%. However, the uptake of ammonium from zooplankton excretion by phytoplankton may have been too fast to result in a measurable concentration, masking the contribution of zooplankton excretion to N availability. Alternatively, we may be underestimating N excretion given that our estimates of zooplankton excretion were not taxon-specific but instead were based on a consolidated dataset of both cladocerans and copepods. This is particularly true when Cladocera dominate in the early and late-summer periods, which could increase community N excretion as Cladocera retain more P than N due largely to their body stoichiometry (Elser *et al.*, 1988). Overall, our estimates of zooplankton excretion were low relative to the concentrations of inorganic nutrients in the ecosystem across the summer; however, they were comparable with other studies using similar allometric equations (Conroy *et al.*, 2005) or direct measurement (den Oude and Gulati, 1988) in eutrophic ecosystems.

In addition to zooplankton, other consumers can play a key role in nutrient recycling in eutrophic ecosystems, particularly detritivores and planktivores such as gizzard shad (Sharitt *et al.*, 2021; Vanni *et al.*, 2006) and mussels (Arnott and Vanni, 1996). However, neither gizzard shad nor zebra mussels have been reported in Green Valley Lake. While we did not quantify the contribution of nutrient recycling by other consumers to availability in Green Valley Lake, these organisms certainly contributed. There is a common carp (*Cyprinus carpio*) population in Green Valley Lake which can influence nutrient cycling through bioturbation and excretion (Weber and Brown, 2009); however, the population is small. We hypothesize that the contributions of fish and other organisms would have a similar seasonality given the large contribution of internal P in the latter half of the season.

Role of zooplankton excretion and grazing on phytoplankton community structure

The redundancy analysis of phytoplankton community composition showed that the daily estimated rate of zooplankton P excretion was related to variation in phytoplankton community composition prior to the cyanobacteria bloom later in summer. This suggests that zooplankton P recycling, in part, influenced phytoplankton biomass and composition. The phytoplankton community was dominated by bacillariophytes and chlorophytes until DOY 172 when cyanophytes dominated the community. This transition is reflected in the discrimination of the phytoplankton community between pre- and post-cyanobacterial dominance in the redundancy analysis (db-RDA). The early summer phytoplankton community was also significantly related to the concentration of inorganic N and total dissolved solids. This corresponds with the seasonal dynamic of nutrient limitation as both chlorophytes and bacillariophytes perform well under P-limitation (Berg *et al.*, 2003). Furthermore, the inorganic N pool was highest in early summer and predominantly composed of nitrate which can be taken up and used by bacillariophytes (Andersen *et al.*, 2020). The higher concentrations of total dissolved solids in the spring are reflective of the input of ions from the watershed with spring melt, including nutrients such as nitrate. These inputs combined with zooplankton excretion drove the community composition in the spring.

Beginning on DOY 172, the phytoplankton community was overwhelmingly dominated by *Microcystis* leading to very stable community composition during mid- and late summer. The mid- to late-summer phytoplankton community was significantly related to temperature and inorganic P concentrations, consistent with other studies describing increasing temperature and N-limitation as key drivers of cyanobacteria dominance (Bogard *et al.*, 2020; Hayes *et al.*, 2020). In fact, diazotrophic cyanobacteria (specifically, *Aphanothece spp.*) did not appear in the Green Valley phytoplankton community until the onset of N-limitation. Other environmental factors were likely influencing the phytoplankton community as the db-RDA described only 41.9% of variation in the phytoplankton community composition. Phytoplankton community turnover is a complex phenomenon driven by a multitude of environmental factors (Wentzky *et al.*, 2020; Sommer *et al.*, 2012), including nutrient and light availability, the latter of which we did not measure. Given the high biomass of phytoplankton, light limitation through self-shading likely played a significant role in phytoplankton dynamics.

While we did not observe significant top-down control of zooplankton on phytoplankton growth based on the Z:P ratios, we did find evidence that zooplankton may have influenced the size structure of the phytoplankton community. The negative relationship between zooplankton length and phytoplankton GALD is consistent with other studies in hypereutrophic lakes indicating that small-bodied zooplankton preferentially graze on small-sized phytoplankton, favoring growth of large filamentous and colonial phytoplankton (Bairagi *et al.*, 2019; Onandia *et al.*, 2015). This is evidenced by the large bloom of *Microcystis* colonies midsummer that drove the increase in phytoplankton GALD we observed in July through early August. It is likely that smaller-bodied zooplankton were contributing, in part, to the dominance of *Microcystis* colonies and higher phytoplankton GALD. By grazing on smaller sized phytoplankton cells or colonies, zooplankton can eliminate smaller phytoplankters leaving a greater proportion of individuals with large GALD to dominate the overall size distribution. The size structure of communities is closely tied to food web structure and energy flow (Brose *et al.*, 2017), indicating that the influence of zooplankton on phytoplankton size structure was influential for the transfer, uptake, and recycling of nutrients by phytoplankton. However, it is unlikely zooplankton were the sole cause of increased phytoplankton GALD as the drawdown of inorganic N we observed midsummer coincided with the bloom of *Microcystis* beginning on DOY 172. Inorganic N is known to promote *Microcystis* growth and was likely influencing the proliferation of *Microcystis* colonies (Chen *et al.*, 2019).

It is also likely that microzooplankton and ciliates played an important role grazing on small phytoplankton species; however, we did not quantify these communities in this study. Furthermore, our phytoplankton counting methods were unable to facilitate the identification of nano- or picophytoplankton species in the water column. Microzooplankton, nano- and picophytoplankton are increasingly recognized as key components of the plankton food web and contribute a significant percentage of grazing pressure on phytoplankton in highly productive ecosystems (Agasild *et al.*, 2007; Zingel *et al.*, 2007). Future studies should examine their seasonal dynamics and potential contribution to ecosystem processes more thoroughly as they can be key components of zooplankton-phytoplankton interactions in nutrient-rich lakes.

CONCLUSIONS

While the importance of consumer-driven nutrient recycling has been demonstrated in less eutrophic waterbodies, the role that zooplankton consumers play in nutrient availability and phytoplankton dynamics in hypereutrophic lakes remained unclear. Our results support a previous comparative study indicating that zooplankton community composition may influence nutrient availability in hypereutrophic ecosystems, as well extend our understanding of the temporal dynamics of zooplankton and phytoplankton interactions. We found evidence of the importance of zooplankton nutrient cycling in a hypereutrophic reservoir with zooplankton excretion providing a large portion of the available P early in the summer, prior to the onset of the cyanobacteria-dominated bloom later in the season. Additionally, zooplankton influenced the early summer phytoplankton community composition through excretion as well as phytoplankton size structure, particularly later in the summer when cyanobacteria were blooming. As demonstrated here, the role of zooplankton nutrient recycling in hypereutrophic lakes is an important component of phytoplankton dynamics and ecosystem function that should be considered in greater detail. Unlike previous assumptions that zooplankton do not contribute substantially to nutrient cycling and phytoplankton dynamics, our results suggest that zooplankton do in fact do contribute to those dynamics, predominantly for a short period early in the summer. Future work should investigate the dynamics of zooplankton nutrient recycling across different climate contexts and over longer time periods, including dynamics through winter and autumn.

ACKNOWLEDGEMENTS

We would like to thank Shania Walker, Halle Rosenboom, Quin Shingai, Rachel Fleck, Elena Sandry, Psalm Amos, Julia Schneller, Adriana Le-Compte, and Ellen Albright for assistance with sample collection and analysis. Additionally, we thank Riley Barbour for assistance with phytoplankton identification and enumeration.

FUNDING

This project was funded by the Iowa Department of Natural Resources and the U.S. Department of Agriculture National Institute of Food and Agriculture (Grant # 2018-09746)**.** This material is based upon work supported by the National Science Foundation Graduate Research Fellowship Program under Grant No. DGE-1747503. Any opinions, findings, and conclusions or recommendations expressed in this material are those of the authors and do not necessarily reflect the views of the National Science Foundation.

DATA ARCHIVING

The data for this study will be archived using the Environmental Data Initiative repository and given a unique digital object identifier. Data will be uploaded in a comma delimited file format with metadata composed of contact information, detailed variable descriptions, complete taxonomic information, temporal resolution, and descriptions for a given variable when appropriate. Metadata will follow the ecological metadata language and be published under a creative commons license. Scripts for data analysis and figure generation will be available and maintained online through GitHub (https://github.com/tjbutts/hyper-plankton) and will eventually be published in Zenodo for long-term storage.

REFERENCES

Agasild, H. *et al.* (2007) Contribution of different zooplankton groups in grazing on phytoplankton in shallow eutrophic Lake Võrtsjärv (Estonia). *Hydrobiologia*, **584**, 167–177.

Ahmed, A. and Wanganeo, A. (2015) Phytoplankton succession in a tropical freshwater lake, Bhoj Wetland (Bhopal, India): spatial and temporal perspective. *Environ. Monit. Assess.*, **187**, 192.

Albright, E. and Wilkinson, G. (2022) Sediment phosphorus composition controls hot spots and hot moments of internal loading in a temperate reservoir. *EarthArxiv*. Preprint.

Andersen, I. M. *et al.* (2020) Nitrate, ammonium, and phosphorus drive seasonal nutrient limitation of chlorophytes, cyanobacteria, and diatoms in a hyper-eutrophic reservoir. *Limnol. Oceanogr.*, **65**, 962–978.

Arnott, D. L. and Vanni, M. J. (1996) Nitrogen and phosphorus recycling by the zebra mussel (Dreissena polymorpha) in the western basin of Lake Erie. *Can. J. Fish. Aquat. Sci.*, **53**, 646–659.

Atkinson, C. L. *et al.* (2017) Consumer-driven nutrient dynamics in freshwater ecosystems: from individuals to ecosystems. *Biol. Rev.*, **92**, 2003–2023.

Bach, S. and Wickham, H. (2020) magrittr: A forward-Pipe Operator for R.

Bairagi, N. *et al.* (2019) Zooplankton selectivity and nutritional value of phytoplankton influences a rich variety of dynamics in a plankton population model. *Phys. Rev. E,* **99**, 012406.

Balseiro, E. G. *et al.* (1997) Nutrient recycling and shifts in N:P ratio by different zooplankton structures in a South Andes Lake. *J. Plankton Res.*, **19**, 805–817.

Berg, G. M. *et al.* (2003) Plankton community composition in relation to availability and uptake of oxidized and reduced nitrogen. *Aquat. Microb. Ecol.*, **30**, 263–274.

Bogard, M. J. *et al.* (2020) Unabated Nitrogen Pollution Favors Growth of Toxic Cyanobacteria over Chlorophytes in Most Hypereutrophic Lakes. *Environ. Sci. Technol.*, **54**, 3219–3227.

Brose, U. *et al.* (2017) Predicting the consequences of species loss using size-structured biodiversity approaches. *Biol. Rev.*, **92**, 684–697.

Chen, Q. *et al.* (2019) Physiological effects of nitrate, ammonium, and urea on the growth and microcystins contamination of Microcystis aeruginosa: Implication for nitrogen mitigation. *Water Res.,* **163**, 114890.

Conroy, J. D. *et al.* (2005) Soluble nitrogen and phosphorus excretion of exotic freshwater mussels (Dreissena spp.): Potential impacts for nutrient remineralisation in western Lake Erie. *Freshw. Biol.*, **50**, 1146–1162.

Cottingham, K. L. *et al.* (2015) Cyanobacteria as biological drivers of lake nitrogen and phosphorus cycling. *Ecosphere,* **6**, 1–19.

Dobberfuhl, D. R. and Elser, J. J. (2000) Elemental stoichiometry of lower food web components in arctic and temperate lakes. *J. Plankton Res.*, **22**, 1341–1354.

Dumont, H. J. *et al.* (1975) The dry weight estimate of biomass in a selection of Cladocera, Copepoda and Rotifera from the plankton, periphyton and benthos of continental waters. *Oecologia*, **19**, 75–97.

Elser, J. and Hassett, R. (1994) A stoichiometric analysis of the zooplankton-phytoplankton interaction in marine and freshwater ecosystems. *Nature*, **370**, 211–213.

Elser, J. J. *et al.* (2000) Pelagic C:N:P Stoichiometry in a Eutrophied Lake: Responses to a Whole-Lake Food-Web Manipulation. *Ecosystems*, **3**, 293–307.

Elser, J. J. *et al.* (1988) Zooplankton-mediated transitions between N- and P-limited growth. *Limnol. Oceanogr.*, **33**, 1–14.

Elser, J. and Urabe, J. (1999) The Stoichiometry of Consumer-Driven Nutrient Recycling: Theory, Observations, and Consequences. *Ecology*, **80**, 735–751.

Erdoğan, Ş. *et al.* (2021) Determinants of phytoplankton size structure in warm, shallow lakes. *J. Plankton Res.*, **43**, 353–366.

Filstrup, C. T. and Downing, J. A. (2017) Relationship of chlorophyll to phosphorus and nitrogen in nutrient-rich lakes. *Inl. Waters*, **7**, 385–400.

Glibert, P. M. *et al.* (2016) Pluses and minuses of ammonium and nitrate uptake and assimilation by phytoplankton and implications for productivity and community composition, with emphasis on nitrogen-enriched conditions. *Limnol. Oceanogr.*, **61**, 165–197.

Guildford, S. J. and Hecky, R. E. (2000) Total nitrogen, total phosphorus, and nutrient limitation in lakes and oceans: Is there a common relationship? *Limnol. Oceanogr.*, **45**, 1213–1223.

Hamre, K. (2016) Nutrient profiles of rotifers (Brachionus sp.) and rotifer diets from four different marine fish hatcheries. *Aquaculture*, **450**, 136–142.

Havens, K. E. and Beaver, J. R. (2013) Zooplankton to phytoplankton biomass ratios in shallow Florida lakes: An evaluation of seasonality and hypotheses about factors controlling variability. *Hydrobiologia*, **703**, 177–187.

Hayes, N. M. *et al.* (2020) Effects of lake warming on the seasonal risk of toxic cyanobacteria exposure. *Limnol. Oceanogr. Lett.*, **5**, 393–402.

Hébert, M. P. *et al.* (2016a) A compilation of quantitative functional traits for marine and freshwater crustacean zooplankton. *Ecology*, **97**, 1081.

Hébert, M. P. *et al.* (2016b) A meta-analysis of zooplankton functional traits influencing ecosystem function. *Ecology*, **97**, 1069–1080.

Hébert, M. P. *et al.* (2017) Linking zooplankton communities to ecosystem functioning: Toward an effect-Trait framework. *J. Plankton Res.*, **39**, 3–12.

Hessen, D. O. *et al.* (2007) RNA responses to N- and P-limitation; reciprocal regulation of stoichiometry and growth rate in Brachionus. *Funct. Ecol.*, **21**, 956–962.

Hillebrand, H. *et al.* (1999) Biovolume calculation for pelagic and benthic microalgae. *J. Phycol.*, **35**, 403–424.

Isles, P. D. F. and Pomati, F. (2021) An operational framework for defining and forecasting phytoplankton blooms. *Front. Ecol. Environ.*, in press.

Karpowicz, M. *et al.* (2020) Effect of eutrophication and humification on nutrient cycles and transfer efficiency of matter in freshwater food webs. *Hydrobiologia*, **847**, 2521–2540.

Karpowicz, M. *et al.* (2021) Transfer efficiency of carbon, nutrients, and polyunsaturated fatty acids in planktonic food webs under different environmental conditions. *Ecol. Evol.*, 1–14.

Legendre, P. and Anderson, M. (1999) Distance-based redundancy analysis: Testing multispecies responses in multifactorial ecological experiments. *Ecol. Monogr.*, **69**, 1–24.

Legendre, P. and Legendre, L. (1998) *Numerical Ecology*. 2nd ed. Elsevier, Amsterdam.

Leroux, S. and Loreau, M. (2015) Theoretical perspectives on bottom-up and top-down interactions across ecosystems. In Hanley, T. and La Pierre, K. (eds), *Trophic Ecology: Bottom-up and top-down interactions across aquatic and terrestrial systems*. Cambridge University Press, pp. 3–27.

Li, Y. *et al.* (2020) Evaluating the phytoplankton, nitrate, and ammonium interactions during summer bloom in tributary of a subtropical reservoir. *J. Environ. Manage.*, **271**, 110971.

Litchman, E. *et al.* (2013) Trait-based approaches to zooplankton communities. *J. Plankton Res.*, **35**, 473–484.

Matsuzaki, S. ichiro S. *et al.* (2018) Bottom-up linkages between primary production, zooplankton, and fish in a shallow, hypereutrophic lake. *Ecology*, **99**, 2025–2036.

McCauley, E. (1984) The estimation of the abundance and biomass of zooplankton in samples. In Downing, J. and Rigler, F. (eds), *A manual on methods for the assessment of secondary productivity in fresh waters*. Blackwell Publishing Ltd, Oxford (UK), pp. 228–265.

Moegenburg, S. M. and Vanni, M. J. (1991) Nutrient regeneration by zooplankton: Effects on nutrient limitation of phytoplankton in a eutrophic lake. *J. Plankton Res.*, **13**, 573–588.

Moody, E. K. and Wilkinson, G. M. (2019) Functional shifts in lake zooplankton communities with hypereutrophication. *Freshw. Biol.*, **64**, 608–616.

Moustaka-gouni, M. and Sommer, U. (2020) Effects of Harmful Blooms of Large-Sized and Colonial Cyanobacteria on Aquatic Food Webs. *Water*, **12**, 1–19.

Oksanen, J. *et al.* (2020) vegan: Community Ecology Package.

Onandia, G. *et al.* (2015) Zooplankton grazing on natural algae and bacteria under hypertrophic conditions. *Limnetica*, **34**, 541–560.

den Oude, P. J. and Gulati, R. D. (1988) Phosphorus and nitrogen excretion rates of zooplankton from the eutrophic Loosdrecht lakes, with notes on other P sources for phytoplankton requirements. *Hydrobiologia*, **169**, 379–390.

Persson, J. *et al.* (2010) To be or not to be what you eat: Regulation of stoichiometric homeostasis among autotrophs and heterotrophs. *Oikos*, **119**, 741–751.

Prater, C. *et al.* (2017) Interactive effects of genotype and food quality on consumer growth rate and elemental content. *Ecology*, **98**, 1399–1408.

R Core Team (2021) R: A language and environment for statistical computing.

Rogers, T. *et al.* (2020) Trophic control changes with season and nutrient loading in lakes. *Ecol. Lett.*, **23**, 1287–1297.

Rönicke, H. *et al.* (2010) Changes of the plankton community composition during chemical neutralisation of the Bockwitz pit lake. *Limnologica*, **40**, 191–198.

Sarnelle, O. and Knapp, R. A. (2005) Nutrient recycling by fish versus zooplankton grazing as drivers of the trophic cascade in alpine lakes. *Limnol. Oceanogr.*, **50**, 2032–2042.

Sharitt, C. A. *et al.* (2021) Nutrient excretion by fish supports a variable but significant proportion of lake primary productivity over 15 years. *Ecology*, **0**, 1–8.

Sommer, U. *et al.* (2012) Beyond the Plankton Ecology Group (PEG) Model: Mechanisms Driving Plankton Succession. *Annu. Rev. Ecol. Evol. Syst.*, **43**, 429–448.

Song, K. and Burgin, A. J. (2017) Perpetual Phosphorus Cycling: Eutrophication Amplifies Biological Control on Internal Phosphorus Loading in Agricultural Reservoirs. *Ecosystems*, **20**, 1483–1493.

Sournia, A. (1978) Phytoplankton Manual. *Monographs on Oceanographic Methodology*. UNESCO, Paris.

Spooner, D. E. *et al.* (2013) Nutrient loading associated with agriculture land use dampens the importance of consumer-mediated niche construction. *Ecol. Lett.*, **16**, 1115–1125.

Sterner, R. W. (1990) The Ratio of Nitrogen to Phosphorus Resupplied by Herbivores : Zooplankton and the Algal Competitive Arena. *Am. Nat.*, **136**, 209–229.

Sterner, R. W. and Elser, J. J. (2002) *Ecological Stoichiometry: The Biology of Elements from Molecules to the Biosphere*.

Stoddard, J. L. *et al.* (2016) Continental-Scale Increase in Lake and Stream Phosphorus: Are Oligotrophic Systems Disappearing in the United States? *Environ. Sci. Technol.*, **50**, 3409–3415.

Striebel, M. *et al.* (2016) Phytoplankton responses to temperature increases are constrained by abiotic conditions and community composition. *Oecologia*, **182**, 815–827.

Teurlincx, S. *et al.* (2017) Species sorting and stoichiometric plasticity control community C:P ratio of first-order aquatic consumers. *Ecol. Lett.*, **20**, 751–760.

Vanni, M. J. (2002) Nutrient cycling by animals in freshwater ecosystems. *Annu. Rev. Ecol. Syst.*, **33**, 341–370.

Vanni, M. J. *et al.* (2006) Nutrient cycling by fish supports relatively more primary production as lake productivity increases. *Ecology*, **87**, 1696–1709.

Wang, M. *et al.* (2019) Seasonal Pattern of Nutrient Limitation in a Eutrophic Lake and Quantitative Analysis of the Impacts from Internal Nutrient Cycling. *Environ. Sci. Technol.*, **53**, 13675–13686.

Weber, M. J. and Brown, M. L. (2009) Effects of Common Carp on Aquatic Ecosystems 80 Years after "Carp as a Dominant": Ecological Insights for Fisheries Management. *Rev. Fish. Sci.*, **17**, 524–537.

Wentzky, V. C. *et al.* (2020) Seasonal succession of functional traits in phytoplankton communities and their interaction with trophic state. *J. Ecol.*, **108**, 1649–1663.

Zingel, P. *et al.* (2007) Ciliates are the dominant grazers on pico- and nanoplankton in a shallow, naturally highly eutrophic lake. *Microb. Ecol.*, **53**, 134–142.

TABLE & FIGURE LEGENDS

Table 1. Statistics for the distance based-Redundancy Analysis (db-RDA) of phytoplankton community composition in Green Valley Lake from May to September 2019.

Figure 1. (A) Zooplankton biomass and community composition and (B) phytoplankton biomass and community composition over the course of the growing season in Green Valley Lake, IA.

Figure 2. (A) Surface water nitrogen and (B) phosphorus concentrations split between total, inorganic, and zooplankton body storage over the course of the growing season. Additionally, (C) surface water molar nitrogen: phosphorus (N:P) ratios split between total and inorganic pools as well as (D) molar N:P ratios of the zooplankton community.

Figure 3. The estimated concentration of total zooplankton community excretion produced over a day compared with the surface water inorganic phosphorus and nitrogen concentrations measured the same day as a percentage. Estimates of zooplankton excretion were derived from published allometric equations of zooplankton body size and excretion rate (Hébert, *et al.*, 2016). The dark lines represent the estimated excretion of either phosphorus or nitrogen, and the shaded area represents the error associated with the estimate for each sampling day.

Figure 4. Distance based-Redundancy Analysis (db-RDA) of the phytoplankton community in Green Valley Lake from May to September 2019. Dots represent sampling points, and the numbers 1-14 are DOY 143, 150, 164, 172, 178, 192, 199, 206, 211, 213, 220, 227, 245, 251, respectively. DOY 245 (13) was omitted from the diagram as there were no available data for inorganic N and P thus the data were omitted from the analysis. The explanatory variables are represented by arrows with significance denoted by an asterisk.

Figure 5. (A) Density ridgeline plots of phytoplankton greatest axial distance (GALD, µm) and zooplankton body size (µm) over the course of the growing season in Green Valley Lake, IA. The black vertical line within each distribution represents the mean. (B) Mean difference between zooplankton length and phytoplankton GALD. DOYs that are missing either phytoplankton GALD or zooplankton length are the result of sample loss or no available data.

TABLES

Table 1.

Permutation test variable	**Sums of Squares**	**pseudo-*F***	***p*-value**
Full model	2.58	2.44	**0.003**
First axis	1.03	5.87	**0.002**
Second axis	0.49	2.76	**0.030**
Inorganic P	0.54	3.07	**0.003**
Inorganic N	0.41	2.32	**0.020**
Zooplankton P excretion	0.58	3.27	**0.004**
Zooplankton N excretion	0.28	1.59	0.099
Temperature (°C)	0.37	2.12	**0.032**
Total Dissolved Solids	0.40	2.28	**0.046**
Residual	1.06		

693 **FIGURES**

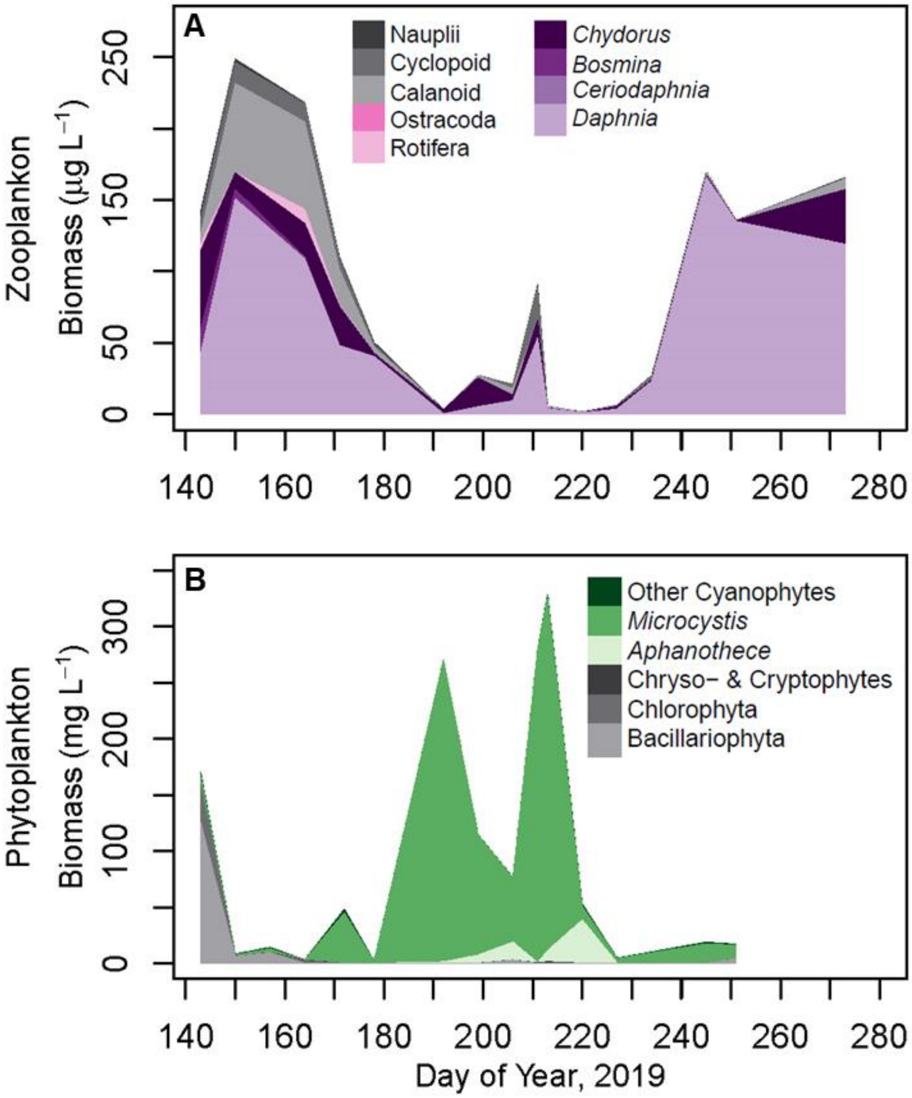

694

695 Figure 1.

696 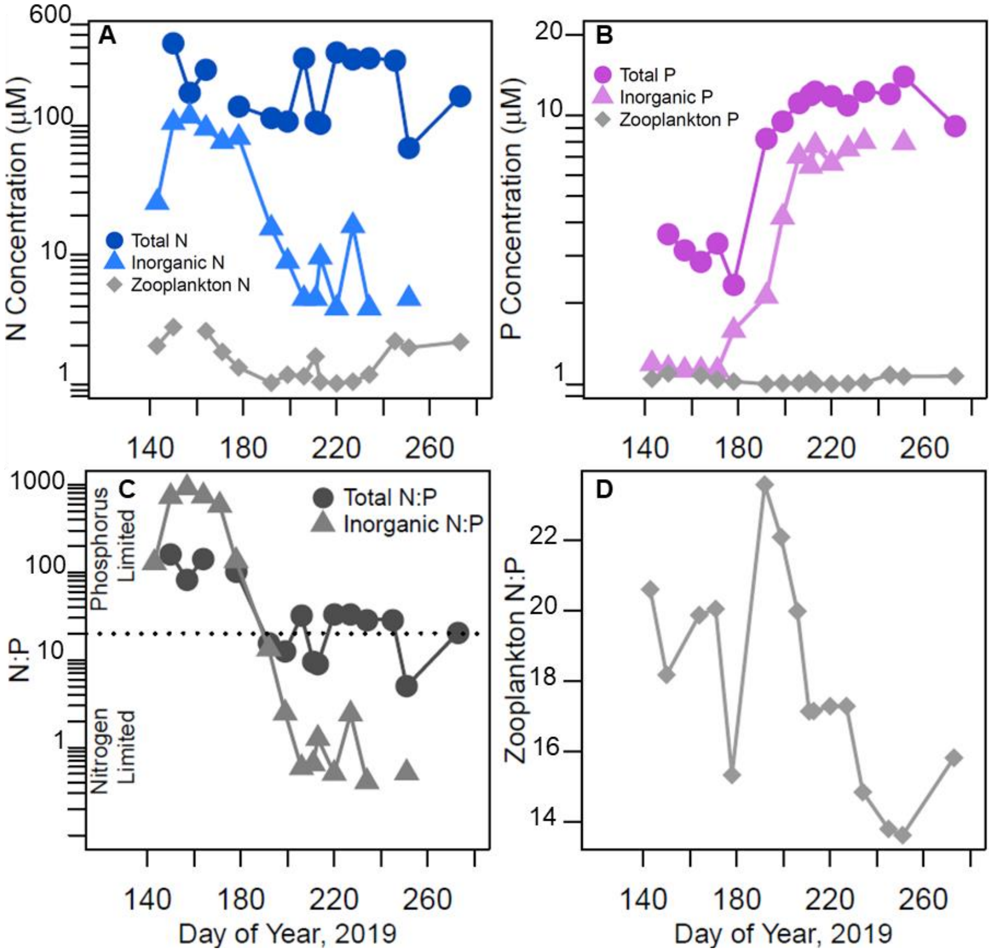

697 Figure 2.

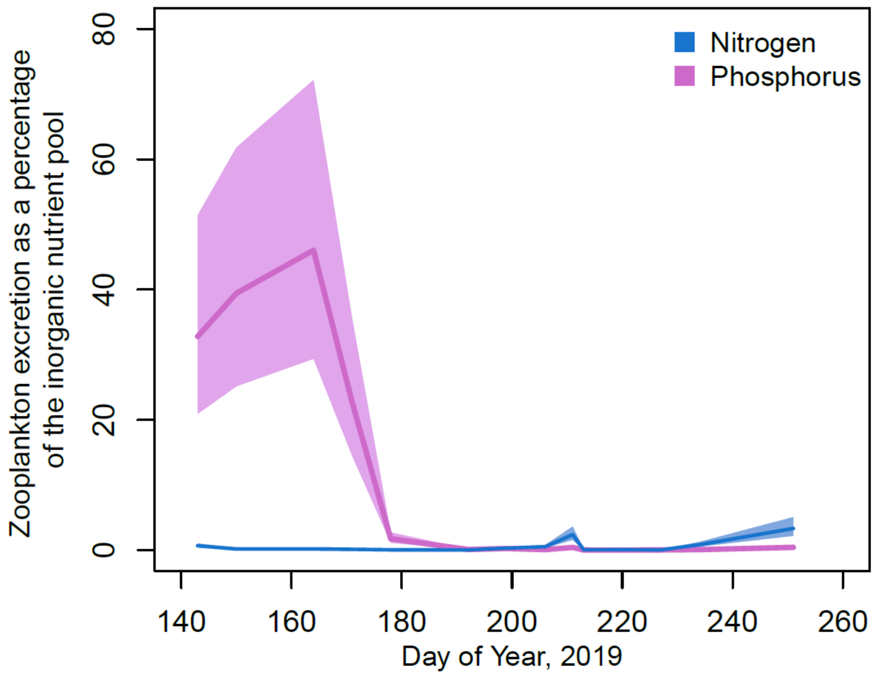
Zooplankton excretion as a percentage of the inorganic nutrient pool
0
20
40
60
80
140
160
180
200
220
240
260
Day of Year, 2019
Nitrogen
Phosphorus

Figure 3.

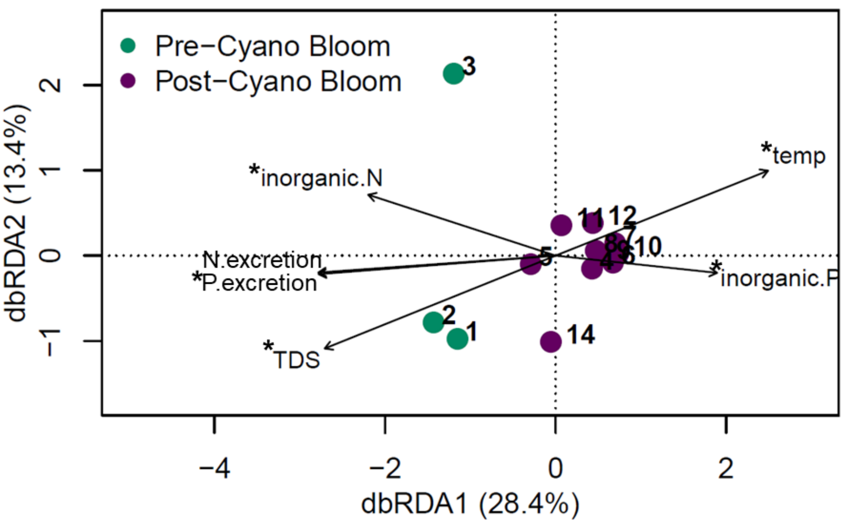
● Pre−Cyano Bloom
● Post−Cyano Bloom
*temp
*inorganic.N
N.excretion
*P.excretion
*inorganic.P
*TDS
1
2
3
4
5
6
7
8
9
10
11
12
14
dbRDA2 (13.4%)
2
1
0
−1
dbRDA1 (28.4%)
−4
−2
0
2

Figure 4.

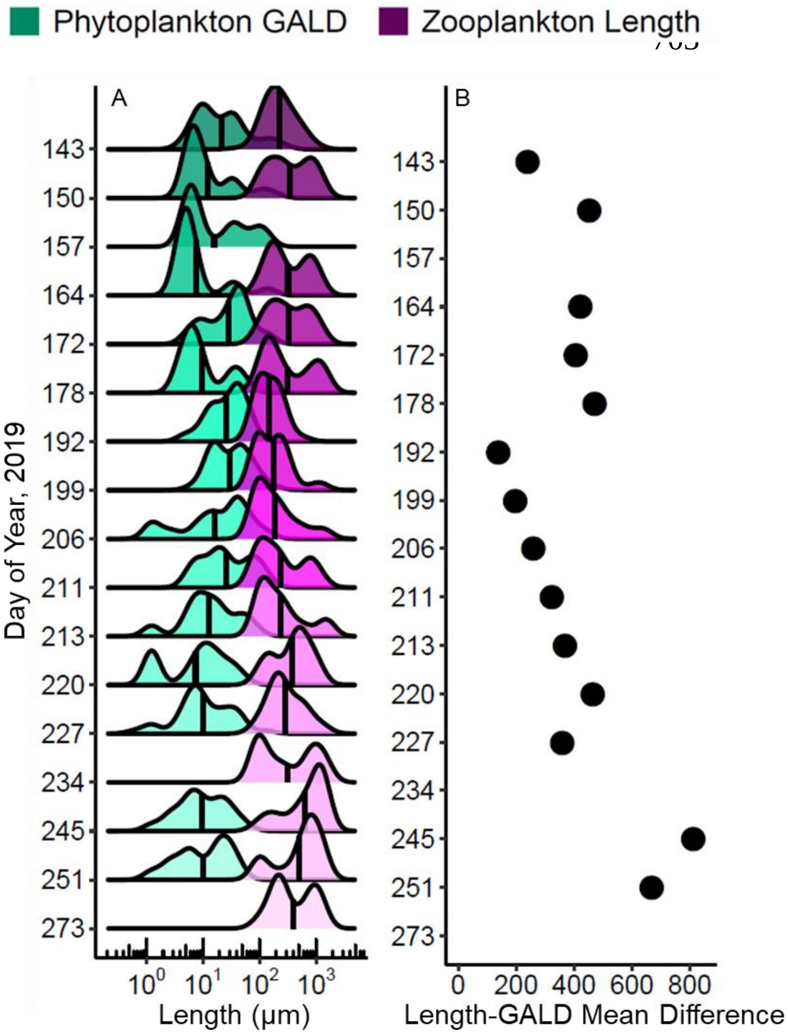
Phytoplankton GALD
Zooplankton Length
A
B
Day of Year, 2019
143
150
157
164
172
178
192
199
206
211
213
220
227
234
245
251
273
10^0
10^1
10^2
10^3
Length (μm)
0
200
400
600
800
Length-GALD Mean Difference

Figure 5.

Supplementary Material

Nutrient concentrations and speciation

The following equations describe how we defined the major fractions of nitrogen (N) and phosphorus (P) in Green Valley Lake. Total N in freshwater is composed organic and inorganic fractions:

$$TN = orgN + DIN \tag{1}$$

where *TN* is total N, *orgN* is organic N in both the particulate (organisms and detritus) and dissolved (urea) form, and *DIN* is dissolved inorganic N composed of *NOx* and *NHx* representing nitrate + nitrite and ammonium + ammonia, respectively. Previous data from the last decade in Green Valley Lake indicated *NHx* were extremely low or undetectable in the surface waters during the summer months. If we assume that *NHx* is undetectable (1) simplifies to:

$$TN = orgN + NOx \tag{2}$$

allowing calculation of *orgN* by rearranging (2):

$$orgN = TN - \ NOx \tag{3}$$

Thus, we could characterize N pools as total (*TN*) representing dissolved and particulate forms of N, organic (*orgN*) representing dissolved organic N (urea) and seston, and inorganic N (*NOx)* representing *DIN* in the surface waters. For our analyses we focused on the TN and DIN pools.

Similarly, P is composed of organic and inorganic fractions in reservoir surface waters:

$$TP = POP \ + \ PIP \ + \ DIP \ + \ DOP \tag{4}$$

where *TP* is total P, *POP* is particulate organic P, *PIP* is particulate inorganic P, *DIP* is dissolved inorganic P, and *DOP* is dissolved organic P. *DIP* and *PIP* were both present within the water column, but our focus for this study was on *DIP* which is far more bioavailable to phytoplankton than *PIP* (Zhou *et al.*, 2005) and thus more influential to nutrient cycling via zooplankton-phytoplankton interactions. Previous data from the last decade in Green Valley Lake indicated *PIP* was extremely low or undetectable in the surface waters during the summer months. Thus, (4) can be simplified by combining *DOP* and *POP* to one organic pool (*orgP*) and using *SRP* as a measure of *DIP* over the course of the growing season:

$$TP = orgP + SRP \tag{5}$$

Therefore, we could characterize P pools as total (*TP*) representing dissolved and particulate forms of P, organic (*orgP*) representing dissolved organic P and seston, and inorganic (*SRP*) representing *DIP* in the surface waters. For our analyses we focused on the TP and SRP pools.

Ammonium + ammonia (NHx) (EPA method 103-A v6) and inorganic suspended solids were measured at the same location in the lake three times during the summer by the Iowa Ambient Lakes Monitoring program (IDNR 2021)**.** Ammonium was analyzed through the alkaline phenate method on a Seal Analytical AQ2 Discrete Analyzer and inorganic particulates were determined via difference between total and volatile suspended solids (USGS method I-3765-85).

Zooplankton excretion equations

Individual zooplankton excretion of P was determined using the following equation from Hébert *et al.*, (2016):

$$ln\left(P_{exc,h}\right) = \ 2.50 + \left(0.84ln(Z_{BS})\right) \tag{6}$$

where $P_{exc,h}$ is excreted P (nM of P individual^{-1} hour^{-1}) and Z_{BS} is the dry mass of an individual zooplankter (mg). Zooplankton excretion of N was determined in a similar manner:

$$ln\left(P_{exc,h}\right) = \ 0.56 + \left(0.70ln(Z_{BS})\right) \tag{7}$$

where $N_{exc,h}$ is excreted N (nM of N individual^{-1} hour^{-1}).

Data were then converted to µM of N or P per day using the following conversions:

$$\frac{nmol\ N\ or\ P}{individual\ \cdot hour} \cdot \frac{24\ hours}{1\ day} \cdot \frac{individuals}{L} \cdot \frac{1\ \mu mol}{1000\ nmol} = \frac{\mu M\ N\ or\ P}{day} \tag{8}$$

The allometric equations were derived from a combined dataset of marine and freshwater zooplankton. Using only the freshwater data did not significantly change the slope, nor was the relationship between excretion and body size significant due to the much smaller sample size. Thus, we only present the combined freshwater and marine model as presented in Hébert *et al.* (2016). Additionally, we used zooplankton excretion equations from Wen and Peters (1994). Specifically, we used their multivariate regression equations for crustacean zooplankton which corrected for temperature (K) and experimental duration (h) in their estimates of excretion. As our data did not have an experimental duration, we dropped the experimental duration correction resulting in the following equations:

$$Log_{10}(P_{exc,wp}) = -5.28 + (0.61 * log_{10}(Z_{BS})) + (0.01 * T) \tag{9}$$

Where $P_{exc,wp}$ is excreted P (µg d^{-1}), Z_{BS} is the body size of an individual zooplankter (µg), and T is water temperature (K).Similarly, for N excretion:

$$Log_{10}(N_{exc,wp}) = -3.47 + (0.74 * log_{10}(Z_{BS})) + (0.00002 * T^2) \tag{10}$$

Where $N_{exc,wp}$ is excreted N (µg d^{-1}), Z_{BS} is the body size of an individual zooplankter (µg), and T is water temperature (K). The pattern of zooplankton excretion was consistent between the two methods; however, the magnitude of excretion was different (Supplementary Table S3).

SUPPLEMENTARY REFERENCES

Hébert, M. P. *et al.* (2016) A meta-analysis of zooplankton functional traits influencing ecosystem function. *Ecology*, **97**, 1069–1080.

Iowa Department of Natural Resources (IDNR) (2021) Water Quality Monitoring and Assessment Section. AQuIA [database].

Wen, Y. H. and Peters, R. H. (1994) Empirical models of phosphorus and nitrogen excretion rates by zooplankton. *Limnol. Oceanogr.*, **39**, 1669–1679.

Zhou, A. *et al.* (2005) Phosphorus adsorption on natural sediments: Modeling and effects of pH and sediment composition. *Water Res.*, **39**, 1245–1254.

Tables

Table S1. Zooplankton genera, order, or class identified over the course of the growing season in Green Valley Lake.

Taxonomic Group	Taxa identified in Green Valley Lake included in grouping
Large Cladocera	*Daphnia* *Simnocephalus* *Ceriodaphnia*
Small Cladocera	*Bosmina* *Chydorus*
Ostracod	Ostracoda
Calanoids	Calanoida
Cyclopoids	Cyclopoida
Nauplii	Copepod nauplii
Rotifers	*Asplanchna* *Keratella cochlearis* *Keratella quadrata* *Pompholyx* *Trichocerca* *Filinia*

Table S2. Phytoplankton genera identified over the course of the growing season in Green Valley Lake.

Taxonomic Group	**Taxa identified in Green Valley Lake included in grouping**
Bacillariophyta	*Asterionella* *Fragilaria* *Stephanodiscus*
	Unknown pennate bacillariophyte
	Unknown centric bacillariophyte
Chlorophyta	*Chalmydomonas* *Coelastrum*
	Cosmarium
	Desmodesmus
	Elakatothrix
	Eudorina
	Monoraphidium
	Oocystis
	Pediastrum
	Schroederia
	Staurastrum
	Unknown chlorophyte
Chyrso - & Cryptophytes	*Mallomonas*
	Cryptomonas
	Komma
Aphanothece (Cyanophyte)	*Aphanothece*
Microcystis (Cyanophyte)	*Microcystis* *Microcystis (Single-celled)*
Other Cyanophytes	*Aphanizomenon*
	Aphanocapsa
	Merismopedia

	Planktolyngbya
	Pseudanabaena
	Snowella
	Woronichinia
	Dolichospermum

Table S3. Estimated zooplankton excretion of N and P (µM d^{-1}) using different published allometric equations from Hébert *et al.* (2016) and Wen and Peters (1994). Uncertainty estimates derived from the allometric equation parameters in Hébert *et al.* (2016) are presented in parentheses.

Zooplankton Excretion (µM N or P day^{-1})

	Nitrogen Excretion		**Phosphorus Excretion**	
DOY	Hébert	Wen & Peters	Hébert	Wen & Peters
143	0.159 (0.143- 0.242)	0.073	0.062 (0.040-0.100)	0.080
150	0.177 (0.116-0.270)	0.082	0.056 (0.036-0.088)	0.072
164	0.167 (0.110-0.255)	0.083	0.058 (0.037-0.091)	0.081
171	0.087 (0.057-0.133)	0.039	0.029 (0.018-0.045)	0.036
178	0.034 (0.022-0.051)	0.014	0.010 (0.007-0.016)	0.012
192	0.003 (0.002-0.004)	0.002	0.001 (0.001-0.002)	0.002
199	0.022 (0.014-0.033)	0.012	0.008 (0.005-0.012)	0.011
206	0.015 (0.010-0.022)	0.007	0.005 (0.003-0.007)	0.006
211	0.068 (0.045-0.104)	0.035	0.023 (0.014-0.035)	0.032
213	0.004 (0.002-0.005)	0.002	0.001 (0.001-0.007)	0.001
220	0.001 (0.001-0.002)	0.001	0.000 (0.000-0.002)	0.001
227	0.005 (0.003-0.007)	0.002	0.002 (0.001-0.003)	0.002
234	0.018 (0.012-0.027)	0.008	0.005 (0.003-0.008)	0.007
245	0.109 (0.072-0.167)	0.046	0.031 (0.020-0.049)	0.037
251	0.095 (0.062-0.145)	0.042	0.029 (0.019-0.046)	0.036
273	0.120 (0.079-0.183)	0.051	0.039 (0.025-0.061)	0.046

Table S4. Potential zooplankton nutrient turnover of various nutrient pools in Green Valley Lake representing the number of days it would take zooplankton excretion alone to meet the water column concentration of total phosphorus, total nitrogen, or inorganic phosphorus on a given sampling day. Missing values were the result of sample loss or the lack of available data and are denoted by NA.

Nutrient Pool	***DOY 143***	***DOY 150***	***DOY 164***	***DOY 172***	***DOY 178***	***DOY 192 - 273***
Soluble Phosphorus	3	3	2	4	57.3	>365

FIGURES

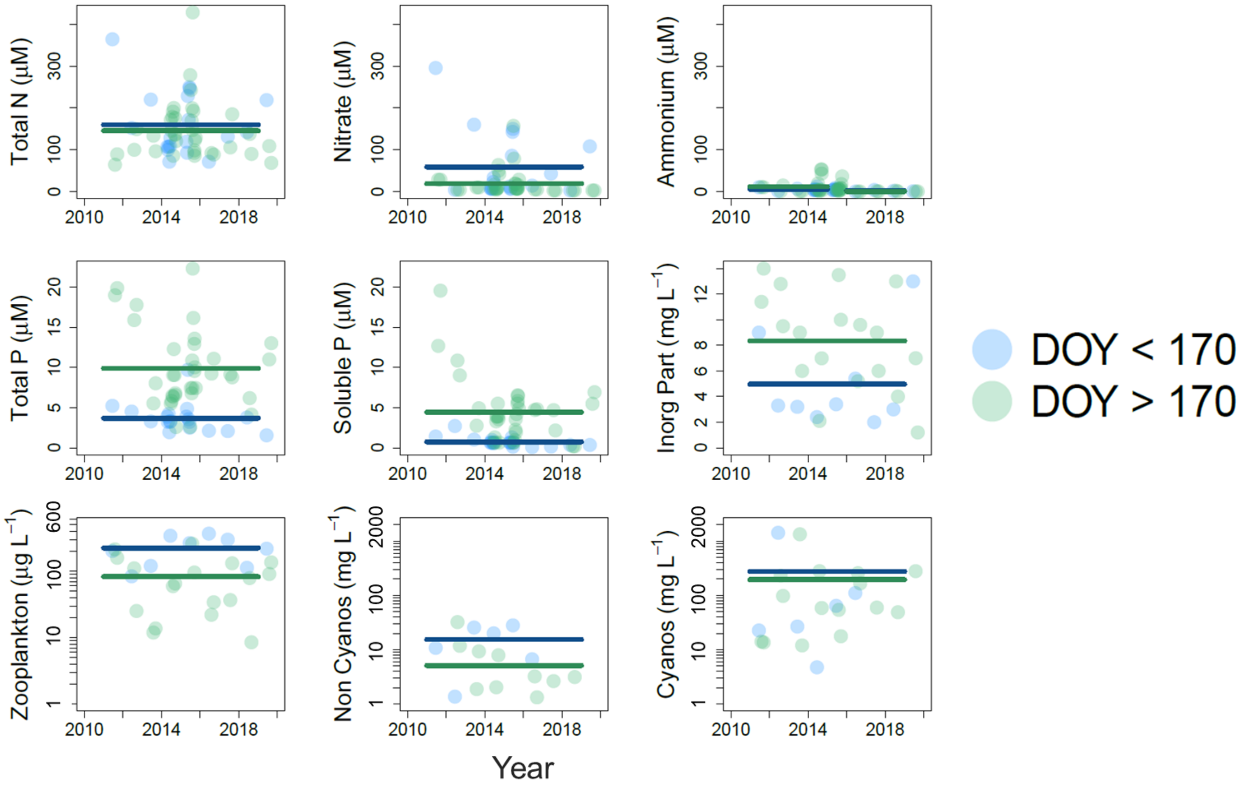

Figure S1. Historical water quality and plankton data for Green Valley Lake. The solid horizontal line is the mean value for the period 2011 – 2019 split between before or after the clear-water period which we determined was around DOY 170 using a breakpoint analysis. From left to right, top to bottom the variables represented are total nitrogen, nitrate, ammonium, total phosphorus, soluble reactive phosphorus, inorganic particulates, zooplankton biomass, non-Cyanophyta biomass, and Cyanophyta biomass. Data were collated from the Ambient Lakes Monitoring program in the state of Iowa (IDNR, 2021). Ammonium concentrations became extremely low or undetectable past 2015 and thus the mean value was split between pre- and post-2015.

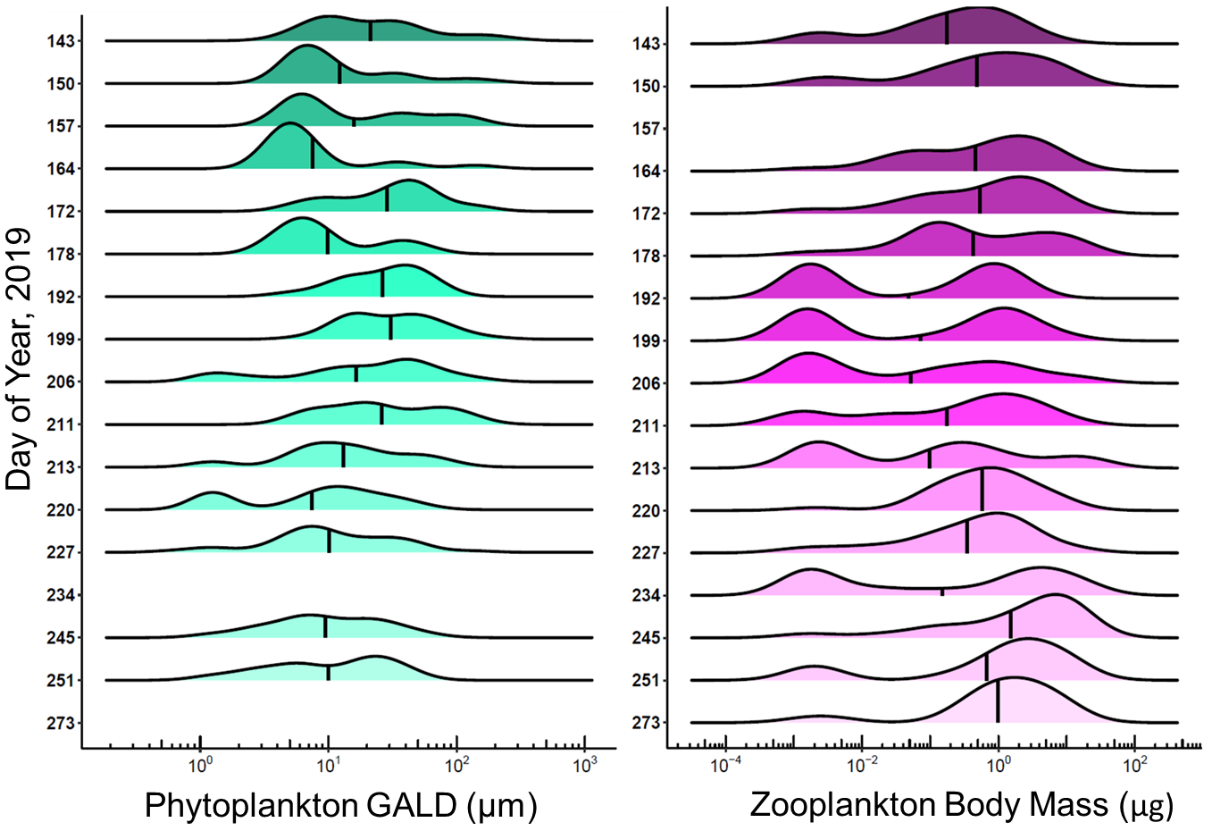

Figure S2. Density ridgeline plots of phytoplankton greatest axial distance (GALD, μm) and zooplankton body mass (μg) over the course of the growing season in Green Valley Lake, IA. The black vertical line within each distribution represents the mean. DOYs that are missing either phytoplankton GALD or zooplankton length are the result of sample loss or no available data.

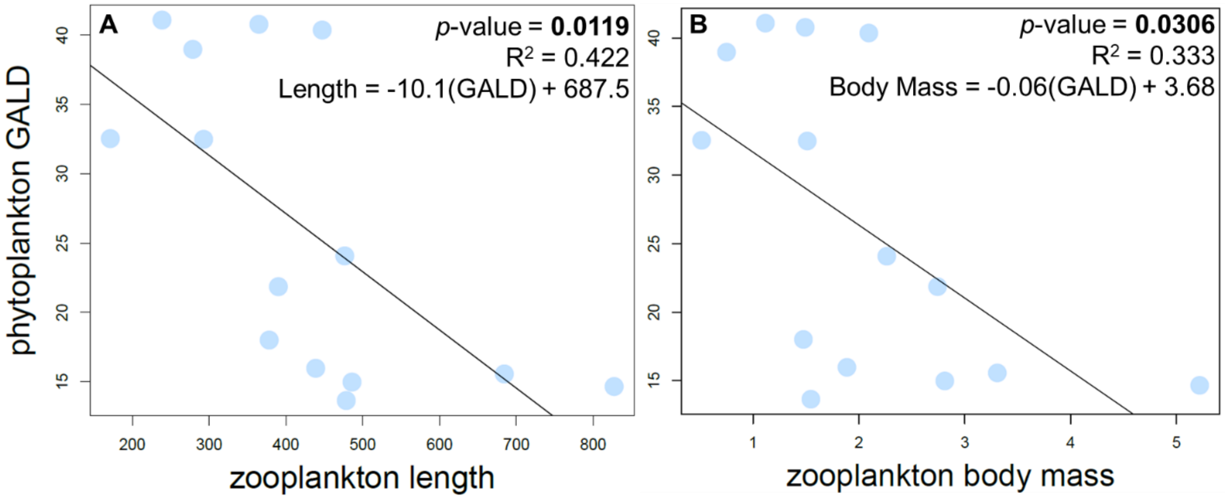

Figure S3. Linear regression of (A) zooplankton body length (µm) and (B) zooplankton body mass (µg) by phytoplankton greatest axial linear distance (GALD, µm).